Available online at www.sciencedirect.com
ScienceDirect
Geochimica et Cosmochimica Acta 70 (2006) 4275–4286
Geochimica
www.elsevier.com/locate/gca

Disorder and the extent of polymerization in calcium silicate and aluminosilicate glasses: O-17 NMR results and quantum chemical molecular orbital calculations

Sung Keun Lee [a,*], Jonathan F. Stebbins [b]

[a] School of Earth and Environmental Sciences, Seoul National University, Seoul 151-742, Republic of Korea
[b] Department of Geological and Environmental Sciences, Stanford University, Stanford, CA 94305, USA

Received 12 December 2005; accepted in revised form 19 June 2006

Abstract

Estimation of the framework connectivity and the atomic structure of depolymerized silicate melts and glasses (NBO/T > 0) remains a difficult question in high-temperature geochemistry relevant to magmatic processes and glass science. Here, we explore the extent of disorder and the nature of polymerization in binary Ca-silicate and ternary Ca-aluminosilicate glasses with varying NBO/T (from 0 to 2.67) using O-17 NMR at two different magnetic fields of 9.4 and 14.1 T in conjunction with quantum chemical calculations. Non-random distributions among framework cations (Si and Al) are demonstrated in the variation of relative populations of oxygen sites with NBO/T. The proportion of non-bridging oxygen (NBO, Ca–O–Si) in the binary and ternary aluminosilicate glasses increases with NBO/T. While the trend is consistent with predictions from composition, the detailed fractions apparently deviate from the predicted values, suggesting further complications in the nature of polymerization. The proportion of each bridging oxygen in the glasses also varies with NBO/T. The fractions of Al–O–Si and Al–O–Al increase with increasing polymerization as CaO is replaced with Al_2O_3, while that of Si–O–Si seems to decrease, implying that activity of silica may decrease from calcium silicate to polymerized aluminosilicates (X_{SiO_2} = constant). Quantum chemical molecular orbital calculations based on density functional theory show that a silicate chain with Al–NBO (Ca–O–Al) has an energy penalty (calculated cluster energy difference) of about 108 kJ/mol compared with the cluster with Ca–O–Si, consistent with preferential depolymerization of Si-networks, reported in an earlier O-17 NMR study [Allwardt, J., Lee, S.K., Stebbins, J.F., 2003. Bonding preferences of non-bridging oxygens in calcium aluminosilicate glass: Evidence from O-17 MAS and 3QMAS NMR on calcium aluminate glass. *Am. Mineral.* **88**, 949–954]. These prominent types of non-randomness in the distributions suggest significant chemical order in silicate glasses that leads to a decrease in silica activity coefficient and will be useful in modeling transport properties of melts.

1. Introduction

The degree of polymerization and network connectivity are among the most critical variables that control the properties of silicate glasses and melts. For instance, the melt viscosity increases several orders of magnitude with decreasing degree of polymerization (e.g., Bottinga and Weill, 1972; Mazurin, 1983; Giordano and Dingwell, 2003). Configurational thermodynamic properties are also affected by the fraction of non-bridging oxygens (NBO). Although they are often not based on spectroscopic and other observations of structure, detailed thermodynamic models of silicate melts have been developed which are often based on structural assumptions (and see Hess, 1995 for review and references).

Because the degree of polymerization plays such an important role in the properties of silicate melts and glasses, it is critical to describe their polymerization states. While there are a number of ways to describe the degree of polymerization, it has often been parameterized with the

* Corresponding author. Fax: +82 2 871 3269.
E-mail address: sungklee@snu.ac.kr (S.K. Lee).

0016-7037/$ - see front matter © 2006 Elsevier Inc. All rights reserved.
doi:10.1016/j.gca.2006.06.1550

mean number of non-bridging oxygen (NBO)/tetrahedron (similar to the classification of crystalline silicates, e.g., for orthosilicates, NBO/T = 4, for chain silicates, NBO/T = 2 etc. e.g., Mysen, 1988) or by the fraction of non-bridging oxygen (X_{NBO}, non-bridging oxygen/total oxygens) that is determined simply from the concentrations of network modifying cations (Ca^{2+}, Na^{+}, etc.) (e.g., Lee, 2005; Mysen and Richet, 2005). Another effective way to describe the degree of polymerization utilizes either an "anion speciation constant" (K_o) based on Temkin's ionic model ($K_o = [O^-]^2/[O^0][O^{2-}]$ where O^-, O^0, and O^{2-} refers to NBO, BO, and metal oxide, respectively) (e.g., Toop and Samis, 1962), or Q species distribution constants (e.g., $K_Q = [Q_n]^2/[Q_{n-1}]\,[Q_{n+1}]$, where Q_n refers to tetrahedral Si groups with n number of bridging oxygens, Masson, 1977; Mysen, 1988). Among these inter-related descriptions of polymerization, parameters are generally based on composition alone, without experimental verification of the structure and speciation, with the possible exception of the Q_n species description. However, X_{NBO} as deduced from composition may not necessarily be consistent with the real X_{NBO} in glasses, as shown by previous O-17 NMR studies of Ca-alumionsilicate glasses where non-negligible fractions of NBO were found for compositions on the charge-balanced join (Ca/Al = 1) (Stebbins and Xu, 1997). Because its fraction can be directly estimated by O-17 NMR, X_{NBO} from O-17 NMR could provide a convenient way to describe the polymerization state more accurately than can be obtained from the composition. To better understand the variation of mechanical, thermodynamic, and transport properties of silicate melts and glasses with the degree of polymerization, it is fundamental to investigate the evolution of their atomic and molecular structures with the degree of polymerization. Here, we explore the structure of calcium silicate and aluminosilicates glasses and melts that have important implications for diverse geological processes in the Earth (e.g., Stebbins et al., 1995; Mysen and Richet, 2005). These systems are also the basis of multi-component glasses that have been widely used in technological applications such as glass fiber composites.

The structures of calcium silicate and aluminosilicate glasses have been extensively studied using various scattering and spectroscopic methods or simulations (see Engelhardt and Michel, 1987; Mysen, 1988; Stebbins et al., 1995; Mysen and Richet, 2005 for review, and McMillan et al., 1982; Merzbacher and Hinggby, 1985; Murdoch et al., 1985; Oestrike and Kirkpatrick, 1988; Eckert, 1992; Stein and Spera, 1995; Stebbins and Xu, 1997; Hwa et al., 1998; Lee and Stebbins, 1999; Petkov et al., 2000; Allwardt et al., 2003; Cormier et al., 2003; Neuville et al., 2004; Iuga et al., 2005; Mysen and Richet, 2005). In general, by replacing Al_2O_3 or SiO_2 with CaO content, the degree of polymerization decreases (i.e., NBO/tetrahedron increases) and the fraction of non-bridging oxygen (NBO) is expected to increase. Details of the cation coordination environments also, of course, have strong implication for their thermodynamic mixing properties. For example, a recent detailed Al-27 3QMAS (triple quantum magic angle spinning) NMR study at high field (17.6 T) quantified the variation in the concentrations of $^{[5]}$Al and $^{[6]}$Al (five- and six-coordinated Al) with composition in the peralkaline $CaO/Al_2O_3/SiO_2$ system (Iuga et al., 2005; Neuville et al., 2006), as previously observed in peralkaline Mg-aluminosilicate and quaternary aluminosilicates glasses (Toplis et al., 2000; Allwardt et al., 2005; Lee et al., 2005). However, detailed atomic and nanoscale structures (e.g., distributions among framework units, $^{[4]}$Si, and $^{[4]}$Al, fractions of NBO) of calcium silicate and aluminosilicate glasses (NBO/T > 0) as a function of NBO/T have not been fully explored. This may be due to broad electromagnetic responses (optical spectroscopy, conventional NMR, and X-ray scattering) from these systems, typical of alkaline earth aluminosilicate glasses.

It has recently been shown that various aspects of structure and disorder of covalent oxide glasses can be determined by exploring their fractions and distributions of oxygen anion environments (Stebbins et al., 2001; Kohn, 2004; Lee, 2005). Element-specific and mostly quantitative solid-state NMR, particularly, O-17 MAS and 3Q (triple quantum) MAS NMR, has been effective in resolving various oxygen environments in aluminosilicate glasses, allowing the detailed quantification of disorder (Kirkpatrick et al., 1986; Dirken et al., 1997; Stebbins and Xu, 1997; Stebbins et al., 1997). This method provides unprecedented resolution of oxygen environments among several element-specific techniques, including X-ray absorption spectroscopy and X-ray photo electron spectroscopy. Ternary aluminosilicate glasses along charge-balanced joins have drawn particular attention and we recently quantified the degree of framework disorder in such glasses (nominal NBO/T = 0) and quantified the degree of Al-avoidance (see below Lee and Stebbins, 2002). Compositional effects on oxygen environments in low silica calcium aluminosilicate glasses with "peralkaline" compositions (NBO/T = 0.6–0.8) have been systematically explored and revealed that the Si–NBO is more energetically favorable than Al–NBO (Allwardt et al., 2003), which is consistent with suggestions from earlier Raman studies (Mysen et al., 1981; Mysen, 1988). The degree of non-randomness in the distribution of NBOs in the peralkaline calcium aluminosilicate would provide key information about configurational thermodynamic and transport properties (Mysen, 1998).

Quantum chemical calculations have provided useful insights into the structure and reactivity of covalent oxide glasses (Tossell, 1993). The structure and energetics of representative oxygen clusters in silicate glasses and melts can be calculated, which helps to predict the properties and to intepret experimental spectroscopic data (e.g., Tossell and Cohen, 2001; Kubicki and Toplis, 2002). While the energetics of bridging oxygen clusters have been explored using quantum chemical methods (Tossell, 1993; Lee et al., 2001), those involving NBOs in calcium aluminosilicate glasses have not been investigated in detail. Calculation

of the relative energetics of various types of NBO would be a useful comparison to the experimental data, and have thus been included here.

Upon describing the various aspects of disorder in the system, we used the following definitions (Mysen and Richet, 2005). "Chemical disorder" is used to describe the distribution of framework units ($^{[4]}$Si and $^{[4]}$Al) and non-framework cations (Ca^{2+}) and is further divided into the degree of framework disorder (distribution of framework units) and the degree of polymerization (defined by X_{NBO}). "Topological disorder" refers to disorder due to bond angle and length distributions (see Richet and Neuville, 1992; Lee, 2005 for more details). It is important to note that the main focus of this paper is the structure of glass, which represents the structure of the supercooled melt as "frozen in" at the glass transition temperature. Implications for the structure of melts can be deduced by thermodynamic modeling of glass structure which includes the effects of temperature. For instance, recent statistical thermodynamic modeling based on quasi-chemical approximations enabled us to predict the structure and the variation in the extent of Si/Al disorder with temperature in aluminosilicates (Lee, 2005). Alternatively, experiments exploring the effect of T_g on glass structure can provide a more direct view of temperature effects on melt structure, and have in fact recently quantitatively confirmed our previous results (Dubinsky and Stebbins, 2005; Dubinsky and Stebbins, 2006).

Here, we explore the structure of Ca-silicate and aluminosilicate glasses with varying NBO/T using O-17 MAS and 3QMAS NMR to provide additional details of the extent of polymerization and disorder. The NBO/T range of the systems (0–2.67) studied here extends from the most polymerized natural melts to well beyond the least polymerized. We also have utilized quantum chemical calculations to investigate the energetics of NBO clusters and preferential depolymerization in silicate networks. We finally discuss the importance of these structural findings for melt properties.

2. Experimental and quantum chemical calculation methods

2.1. Sample preparation

Ca-silicate and aluminosilicate glasses were synthesized from mixtures of oxide (Al_2O_3, 40% O-17 enriched SiO_2) and $CaCO_3$ reagents (Stebbins and Xu, 1997). About 0.2 wt% Co oxide was added to enhance spin–lattice relaxation and thus reduce total NMR signal acquisition time. The mixtures (typically about 250 mg) were decarbonated at around 800 °C and fused at about 1500–1670 °C (above the melting temperature) in Ar for an hour and then quenched. Negligible weight loss was observed after considering decarbonation. The nominal compositions of the binary calcium silicate glasses are $CaO/SiO_2 = 4:3$ (CS43) and $CaO/SiO_2 = 38.5:61.5$ mol% (CS46, Lee and Stebbins, 2003b). Those of the calcium aluminosilicate glasses are, CAS312 ($CaO/Al_2O_3/SiO_2 = 3:1:2$ mole ratio), relatively depolymerized CAS313 (grossularite garnet composition $CaO/Al_2O_3/SiO_2 = 3:1:3$), and CAS223 ($CaO/Al_2O_3/SiO_2 = 2:2:3$), which is on the charge-balanced join. The melts were quenched into glasses by dipping a Pt crucible into water. The resulting glasses were optically transparent and no evidence for the presence of crystalline phases was found under polarizing microscope. While we have not done probe analysis for the sample and the sample may be chemically heterogeneous, the weight loss during synthesis is negligible considering decarbonation, suggesting that the resulting glass composition should be close to the nominal values.

2.2. NMR spectroscopy

O-17 NMR experiments (9.4 and 14.1 T) were performed on a modified Varian VXR-400s spectrometer (9.4 T) and Varian Inova 600 (14.1 T) with a Doty Scientific, Inc. MAS probe (4 mm silicon nitride rotor) and a Varian T3 probe (3.2 mm zirconia rotor), respectively. O-17 MAS NMR spectra were collected with single pulse acquisition with a pulse length of 0.25 μs (about 15° radio frequency tip angle for solids), a recycle delay of 1 s with 15 kHz spinning speed at 9.4 T, and 0.15 μs pulse, recycle delay of 1 s, and 18 kHz spinning speed at 14.1 T. O-17 3Q MAS NMR spectra at 9.4 T were collected using shifted-echo pulse sequences as previously described (5.25 μs-delay–1.75 μs-delay–20 μs) with recycle delays up to 10 s for calcium aluminosilicate glasses. O-17 NMR frequencies are reported relative to 20% O-17 water as an external standard. Detailed information on NMR conditions can be found in our previous reports (Lee et al., 2001; Lee and Stebbins, 2002). Here the O-17 3QMAS NMR spectra were processed with a shear transformation with isotropic dimension frequencies scaled as described by earlier study, using the software package "RMN" (P. Grandinetti, Ohio State University) (Baltisberger et al., 1996).

2.3. Quantum chemical molecular orbital calculations

Quantum chemical molecular orbital calculations (geometry optimization and single point energy) were performed on model Ca-aluminosilicate clusters to explore the energetics of non-bridging oxygen distribution in calcium aluminosilicate glasses with Gaussian98 (Foresman and Frisch, 1996; Frisch et al., 1998). The three clusters studied are a chain aluminosilicate ($CaAl_2Si_1O_2(OH)_8$) where all the oxygens are BO, a cluster with 1 NBO on Si ($CaAl_2Si_1O_2O_{Si-NBO}(OH)_7$), and a cluster with 1 NBO on Al ($CaAl_2Si_1O_2O_{Al-NBO}(OH)_7$). All the oxygens except bridging oxygens (Si–O–Al and Al–O–Al) were terminated with hydrogen for charge balance. The geometry of each cluster was optimized at the Hatree-Fock (HF) level of theory with a 6-311G(d) basis; the single point energy was then calculated at the B3LYP level of theory with the 6-311G(2d,p) basis set with local density approximations. Upon optimizing the geometry of each cluster, bond lengths (Si–O, Al–O,

Al–OH) and angles (Al–O–H and Si–O–H) in each cluster were fixed while other internal variables (e.g., Si–O–Al and Al–O–Al angle and Ca–O distance) are allowed to be fully relaxed (see below for limitations of these approaches). The purpose of these quantum chemical molecular orbital calculations is to yield *qualitative* theoretical interpretation of the relative stability among NBOs (i.e., Ca–O–Si and Ca–O–Al), as Ca–O–Al is not present in the glasses described here. Future modeling efforts with varying Ca/Al ratio (number of Ca around NBO and BO as well as Si/Al ratio) and with larger clusters would provide a more quantitative description of the experimental spectra.

3. Results and discussion

3.1. O-17 MAS and 3QMAS NMR

3.1.1. Binary calcium silicate glasses

Fig. 1 shows O-17 MAS NMR spectra for binary calcium silicate glasses with varying CaO/SiO_2 ratio [at 14.1 (A) and 9.4 T (B)] where a non-bridging oxygen peak (a narrow component around 100 ppm, Ca–O–Si) and a bridging oxygen peak (a broad component around 30–50 ppm, Si–O–Si) are clearly resolved. The proportion of NBO in the binary calcium silicate glasses increases with increasing CaO content from about 50% (CS46) to 79% (CS43) (obtained from by fitting MAS NMR spectra with two Gaussian functions) as expected from the stoichiometry (50% and 80%, respectively).

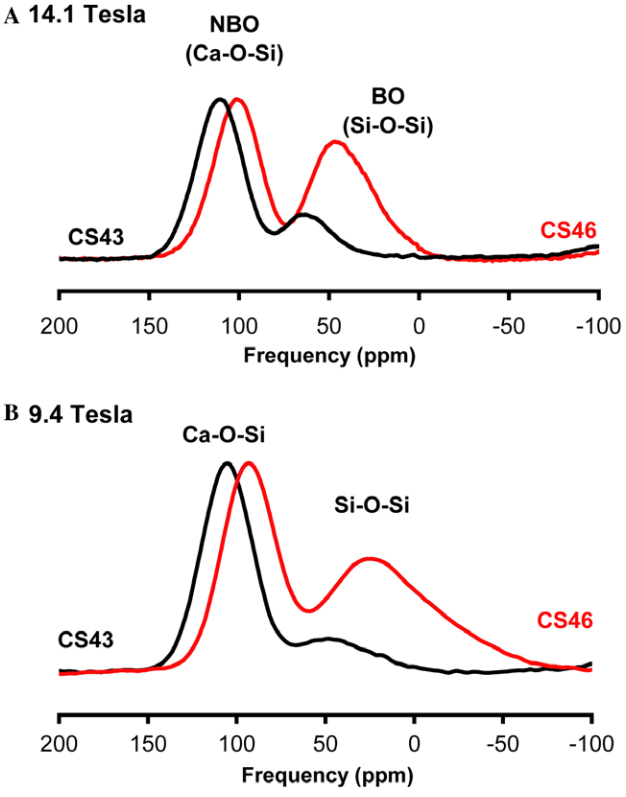

Fig. 1. ^{17}O MAS spectra for binary calcium silicate glasses $CaO/SiO_2 = 4{:}3$ (CS 43) and $CaO/SiO_2 = 4{:}6$ (CS 46) at 14.1 T (A) and 9.4 T (B).

NBO and BO peak positions move toward higher frequency (larger chemical shift) with increasing CaO content. For instance, the NBO peak position for CS46 is about 100 ppm and that of CS43 is centered at around 109 ppm (at 14.1 T, Fig. 1B). These changes could stem from both variations of isotropic chemical shift (δ_{iso}) and quadrupolar coupling constant (C_q). Those NMR parameters for CS46 were previously reported, with δ_{iso} of 104.7 (±2 ppm) and C_q (assuming that quadrupolar asymmetry parameter η is 0.5) of about 2.1 MHz (Lee and Stebbins, 2003b). Those for CS43 obtained from 3QMAS NMR (see below) are δ_{iso} of 116 (±2 ppm) and C_q ($\eta \approx 0.5$) of about 2.1 MHz. The variation of NBO peak position with composition is, therefore, mostly due to changes in isotropic chemical shift. This variation with Ca/Si suggests some change in atomic configurations around the NBO. According to "the perturbed distribution of network modifying cations" (extension of the "perturbed Na distribution model," Lee and Stebbins, 2003a), Ca cations would see an average NBO/BO ratio in their proximity (i.e., mostly the first coordination shell), where the average Ca–O distance is shorter for Ca–NBO than Ca–BO (a similar trend can account for Na NMR spectra for Na-silicates and aluminosilicates). Therefore, with increasing Ca content, Ca "sees" oxygens in a higher NBO/BO ratio, lowering the average Ca–NBO distance. This could lead to an increase in Si–O bond length. Recent NMR studies of crystalline chain silicates reported that O-17 isotropic chemical shifts do tend to increase with Si–NBO bond length (Ashbrook et al., 2002), which could account for the trend observed here for NBO.

BO clusters (Si–O–Si) are likely to show a similar trend: the O-17 δ_{iso} of Si–O–Si appears to increase with CaO content. This trend may be due to an increasing number of Ca around BO as also has been reported for Ca-aluminosilicate glasses on the charge-balanced join (Lee and Stebbins, 2000), and is consistent with that reported for binary sodium silicate glasses (Xue et al., 1994). Our recent quantum chemical calculations of sodium aluminosilicate rings also predict that oxygen chemical shift increases with increasing Si–O bond length in bridging oxygens (Lee, 2004).

3.1.2. Calcium aluminosilicate glasses

Fig. 2 presents O-17 MAS NMR spectra for Ca-silicate and Ca-aluminosilicate glasses in the CS43–CAS223 pseudobinary join where the degree of polymerization from stoichiometry (e.g., $X_{CaO} - X_{Al_2O_3}$) gradually increases. The Al-free Ca-silicate glass [CS43, $X_{CaO} = CaO/(CaO + Al_2O_3) = 1$] has a larger fraction of NBO (Ca–O–Si) that decreases with increasing Al content to CAS313 ($X_{CaO} = CaO/(CaO + Al_2O_3) = 0.75$) and CAS223 ($X_{CaO} = 0.5$). There is a non-negligible fraction of NBO in the CAS223 glass as previously reported in the other charge-balanced (Ca/Al = 1) calcium aluminosilicate glasses (Stebbins and Xu, 1997; Stebbins et al., 1999; Lee and Stebbins, 2002; Oglesby et al., 2002). Note that the NBO peak in the

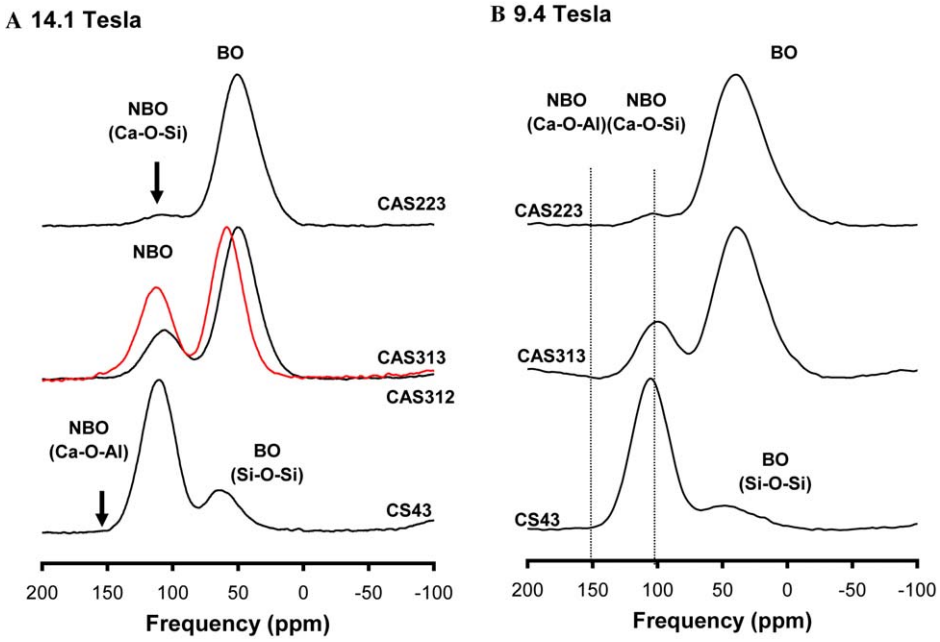

Fig. 2. ^{17}O MAS NMR spectra (9.4 T) for calcium aluminosilicate glasses on the calcium silicate–calcium aluminosilicate join at 14.1 T (A) and 9.4 T (B). Spectrum with red color refers to CAS312.

spectra of CAS223 and CAS313 glasses corresponds to predominantly Ca–O–Si (around 100 ppm). A recent O-17 NMR study of peralkaline, silica-poor Ca aluminosilicate glasses showed that Ca–O–Al can be observed exclusively at very high Al/Si ratios and its δ_{iso} is about 150 ppm (Allwardt et al., 2003). While there could be a few % of Ca–O–Al in CAS313, its presence is not clear. While the proportions of the three types of BO (Si–O–Si, Si–O–Al, and Al–O–Al) cannot be uniquely obtained from O-17 MAS NMR, the fraction of total BO clearly does increase with Al content and the extent of polymerization.

As has been previously demonstrated, two-dimensional 3QMAS NMR (Frydman and Harwood, 1995; Medek et al., 1995; Amoureux et al., 1996) provides improved resolution among oxygen clusters over one-dimensional MAS NMR (e.g., Dirken et al., 1997; Stebbins and Xu, 1997). Fig. 3 shows O-17 3QMAS NMR spectra for the CS43–CAS223 series where the variation of populations of NBO clusters as well as BOs with X_{CaO} are clearly shown and thus reflect the effects of the degree of polymerization. Fig. 3b shows the ranges of peak positions in the spectrum for CAS313, where there is considerable peak overlap among the different types of bridging oxygens, unlike in previous results for alkali aluminosilicates (e.g., Dirken et al., 1997; Lee and Stebbins, 2000). The peak position for each bridging oxygen site as drawn with ellipses in the 2D NMR spectra (Fig. 3B) does not vary much with composition in Ca-aluminosilicate glasses. The Ca–O–Si peak is well resolved at around 100 ppm in the MAS dimension and −67 ppm in the 3QMAS dimension. The NBO fraction (Ca–O–Si) decreases with decreasing X_{CaO}, consistent with O-17 MAS NMR results (Fig. 2). BO clusters [Si–O–Si (−50 ppm in the 3QMAS isotropic dimension), Si–O–Al (at about −40 ppm in the isotropic dimension), and Al–O–Al] are partially resolved. Qualitatively, it is clear that the fractions of Si–O–Al and Al–O–Al increase with increasing Al and decreasing X_{CaO} from CS43 to CAS223 while the proportion of Si–O–Si appears to decrease with decreasing X_{CaO}, all as expected from the composition (see below for quantification of oxygen site populations). Fig. 4 shows the total isotropic projections of the O-17 3QMAS NMR spectra for the glasses on the CS43–CAS223 join, where similar variations of oxygen cluster populations are observed. Total isotropic projection (sum of data along the lines parallel to the MAS axis) allows us to have higher S/N than in an individual slice.

While some effects of composition on the structure (e.g., Al coordination) in calcium aluminosilicate glasses has been extensively studied, the changes in oxygen anion environments remain to be explored in detail. Fig. 5 shows the O-17 3QMAS NMR spectrum for the partially depolymerized Ca-aluminosilicate glass, CAS312 ($CaO/Al_2O_3/SiO_2 = 3:1:2$). Compared with CAS313, the NBO (Ca–O–Si) fraction is clearly larger and the proportion of Al–O–Al is also more prominent. The Si–O–Si fraction is obviously smaller for CAS312. Fig. 6 shows the total isotropic projection for the CAS312 and CAS313 glasses, manifesting the changes in oxygen cluster fraction and environments with X_{SiO_2}.

Finally, while it is not directly relevant to the structure-property relations of the CS and CAS glasses, it is worth noting the effects of the external magnetic field on the spectra, which are one of the fundamental aspects of solid-state NMR of quadrupolar nuclei including O-17 (e.g., Kohn et al., 1998; Gan et al., 2002; Stebbins et al., 2002). Recent high field NMR studies of quadrupolar nuclides yield

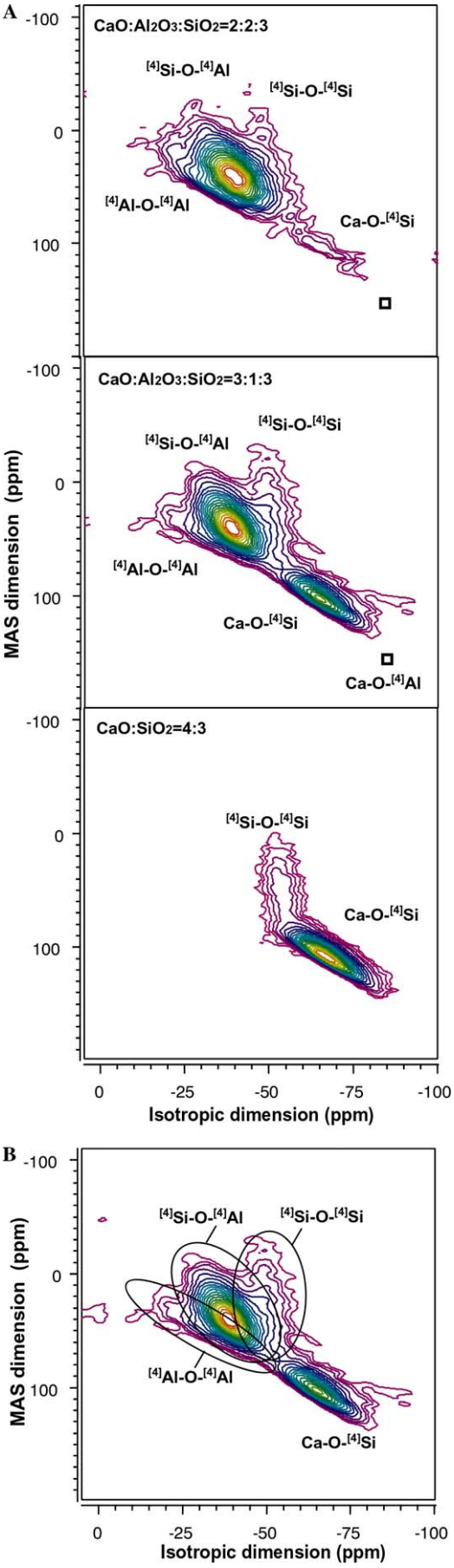

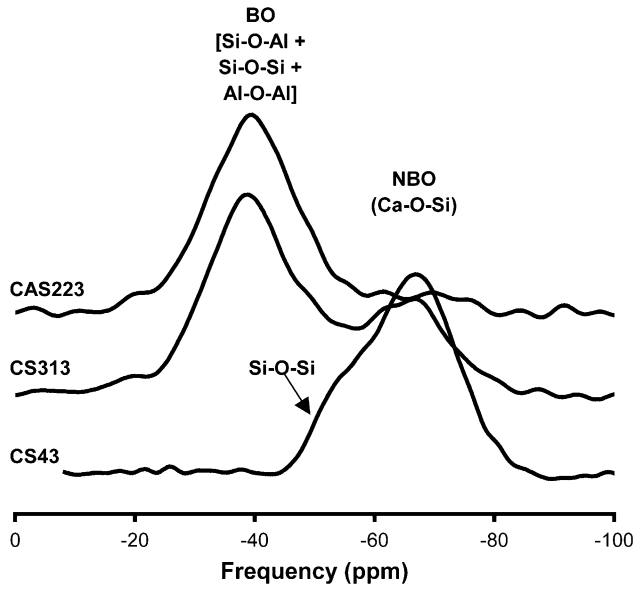

Fig. 4. Total isotropic projections of O-17 3QMAS spectra (9.4 T) of glasses along the CS43–CAS223 join.

improved resolution in the spectra with reduced perturbation by quadrupolar broadening. Fig. 7 shows O-17 MAS NMR spectra for the two calcium silicate binary glasses at both 9.4 T and 14.1 T (Reorganized from Figs. 1 and 2) demonstrating the effect of magnetic field on the peak shape and positions. The peak positions move to higher frequency with increasing field, as the 2nd order quadrupolar shift and broadening decreases. Because the C_q of NBO (about 2.1 MHz) is smaller than that of BO (about 4.5 MHz), the effects of increasing the external field are considerably more prominent for the latter.

3.2. Degree of polymerization and framework disorder

Framework disorder in aluminosilicate silicate glasses and melts depends on temperature, composition and probably pressure. With increasing temperature, the deviation from a random distribution among framework units decreases (Dubinsky and Stebbins, 2005; Lee, 2005; Dubinsky and Stebbins, 2006). The field strength of the modifier cation(s) has been identified as one of the important factors controlling the extent of chemical disorder, as suggested both spectroscopically and thermodynamically (e.g., Navrotsky et al., 1982; Murdoch et al., 1985; Mysen, 1988; Hess, 1995; Navrotsky, 1995). The degree of polymerization is a convenient parameter with which the atomic and nanoscale structures and the macroscopic properties can be described. O-17 NMR probes the fraction of non-bridg-

Fig. 3. (A) ^{17}O 3QMAS NMR spectra (9.4 T) for Ca-silicate and aluminosilicate glasses along the CS43–CAS223 join. Contour lines are drawn from 8 to 98% of relative intensity with a 5% increment and an added line at 4%. (B) ^{17}O 3QMAS NMR spectrum for CAS313 where three ellipses for the oxygen clusters were added to roughly show the contributions from the various oxygen species as discussed in the text.

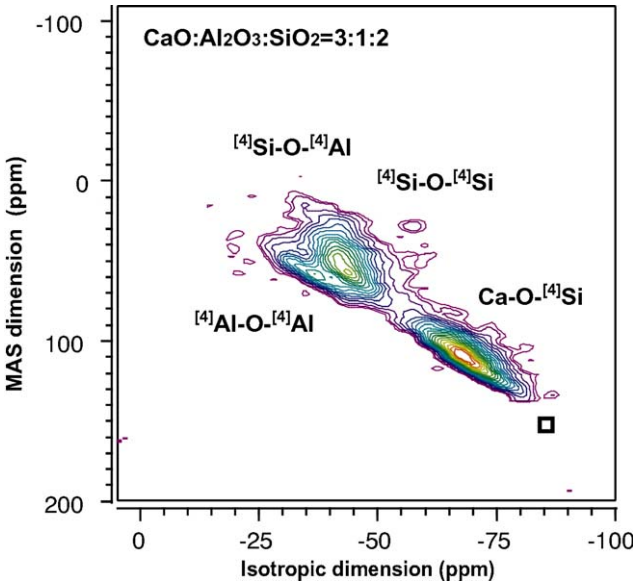

Fig. 5. ^{17}O 3QMAS NMR spectrum for $CaO/Al_2O_3/SiO_2 = 3:1:2$ glass at 9.4 T. Open square shows the center of the peak position for Ca–O–$^{[4]}$Al (Allwardt et al., 2003). Contour lines are drawn from 8 to 98% of relative intensity with a 5% increment and an added line at 4%. See also Fig. 3B caption for the ranges of peak position for each bridging oxygen.

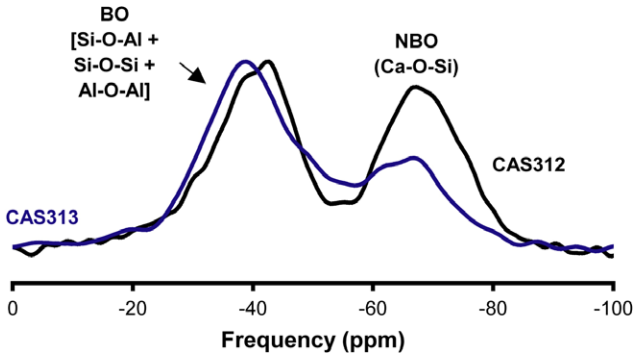

Fig. 6. Isotropic projection of the ^{17}O 3QMAS NMR spectra (9.4 T) for CAS 312 and 313 glasses.

ing oxygen and thus can directly characterize the degree of polymerization. In order to better constrain the macroscopic properties, estimation of the fractions of all the oxygen clusters is important. Fig. 8 shows the oxygen cluster populations for glasses on the CS43–CAS223 join as a function of NBO/T. Here, the fraction of Ca–O–Si was quantified from O-17 MAS NMR as previously mentioned. Then, the total isotropic projections of the O-17 3QMAS NMR spectra the glasses in the CS43–CAS223 were fitted using four Gaussian functions representing each NBO and BO cluster.

Because of the considerable peak overlap for the CS43–CAS223 glasses, we describe this fitting procedure in some detail. Several types of constraints were applied. The position and width of the Ca–O–Si (NBO) peak are relatively well constrained by the spectrum for CS43. These were thus used in fitting the data for the aluminosilicates, with small

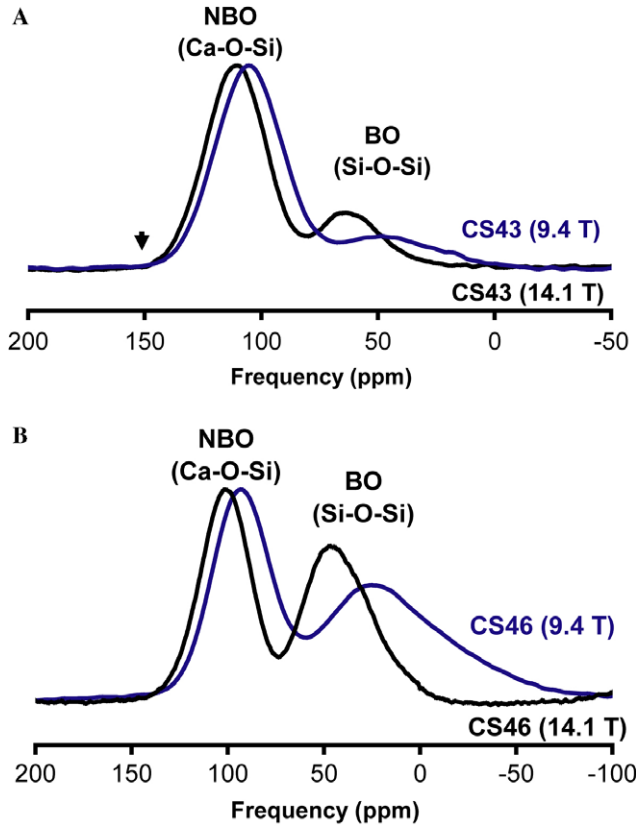

Fig. 7. Effect of external magnetic field on the O-17 MAS NMR spectra for Ca-silicate glasses (14.1 T and 9.4 T). (A) CS43 and (B) CS46.

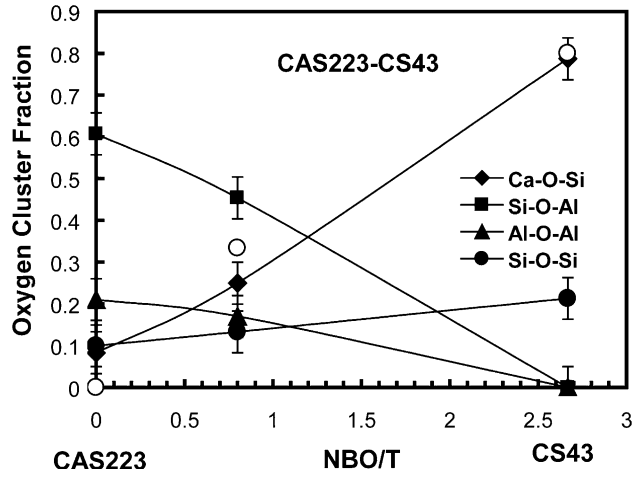

Fig. 8. Variation of oxygen cluster populations with varying degree of polymerization (NBO/T, or $CaO/(CaO + Al_2O_3)$). Open circle denotes calculated NBO fraction from composition.

ranges of variation allowed for compositional effects: -67.5 ± 2 ppm for the position and 7 ± 1 ppm for the width. The initial Si–O–Si peak positions and widths were also obtained from the two-dimensional 3QMAS spectrum of CS43, and were constrained to be -54 ± 2 ppm and 3.7 ± 0.7 ppm for the ternary compositions. The Al–O–Al peak position was from our previous report (Lee and Steb-

bins, 2002) for charge-balanced Ca-aluminosilicate glasses with low Si/Al ratio of 0.5 and thus high contents of this species, and was fixed at −34 ppm in initial fitting, with 7 ± 1 ppm width. The initial estimate of the Si–O–Al peak position (−40 ppm) is also from the previous paper (Lee and Stebbins, 2002) and allowed to vary within ±3 ppm, with the width as 6 ppm ± 2 ppm. With these constraints, the isotropic spectra for CAS223 and CAS313 were then fitted simultaneously, using the same component positions and widths for both. We then fitted the spectra again after removing the constraint on −34 ppm for the Al–O–Al peak position, improving the fit. Results were given in Fig. 9. Due to the peak overlap, the fits are rather non-unique and represent one of the many possible solutions. The X_{Si}'s (=Si/(Si + Al)) for CAS223 and CAS313 are 0.43 and 0.6, respectively while those obtained from the fitting results are 0.46 (CAS223) and 0.54 (CAS313), suggesting that the fitting result is not "perfect" and this slight deviation is due to the fact that the peak positions and widths are fixed in the fitting. However, they at least represent a plausible and consistent model of the distribution of oxygen species as a starting point for discussion and future studies. We note that fitting of the 2D spectrum (instead of fitting the 1D projection) would be desirable if the peak overlap among oxygen clusters is significant (Massiot et al., 2002). Our routine here using Gaussian functions for the fitting of the 1D isotropic projections is identical to 2D fitting with an assumption of a Gaussian peak shape for each oxygen cluster. The actual peak shape may deviate from Gaussian and thus contribute to the sources of uncertainty in the calculated intensity as previously mentioned.

Because the relative peak intensities in 3QMAS NMR depend to some extent on the experimental conditions as well as the quadrupolar interactions (e.g., C_q), the 3QMAS signal intensity of each peak was calibrated considering all the experimental details (power and duration of pulses, delays, and quadrupolar interactions) (Medek et al., 1995; Wu et al., 1996; Massiot et al., 2002; Lee and Stebbins, 2003a). The methods used were described previously (Bak et al., 2000) and were applied in earlier studies (Lee and Stebbins, 2003a; Lee, 2004). The differences in NBO fractions in the glasses obtained here from the MAS vs. the calibrated 3QMAS intensities (considering C_q dependences of the NBO and BO) are quite small, suggesting the calibrations were reasonably accurate. Because C_q values for the NBO are considerably lower than those for BO, the 3QMAS intensities of the former are over-represented by roughly 10% for the experimental conditions used here. We note that for higher pulse power and external fields, comparisons of O-17 data for borosilicate glasses have yielded experimental corrections that were small enough with respect to experimental error to be not included (Du and Stebbins, 2005).

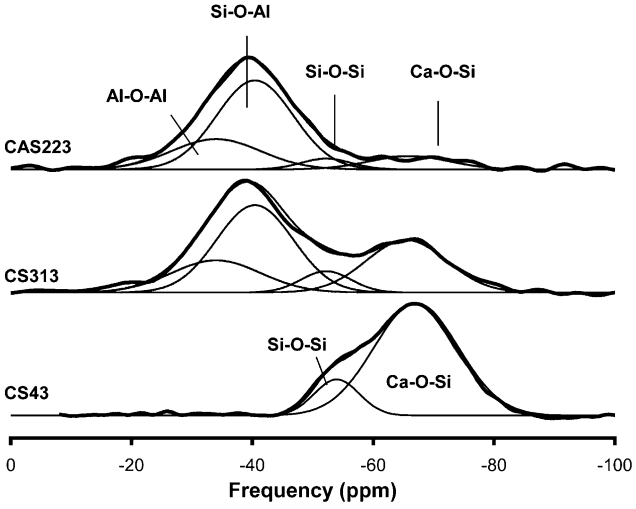

Fig. 9. Fitting results of total isotropic projections for O-17 3QMAS NMR spectra for CS43–CAS223 join, as discussed in detail in the text.

Calibrated NBO fractions along the CS43–CAS223 join increase with increasing NBO/T from about 8% [NBO/T = 0, $CaO/(CaO + Al_2O_3) = 0.5$] to 79% [NBO/T = 2.667, $CaO/(CaO + Al_2O_3 = 1)$]. While the fraction of NBO for the binary calcium silicates as well as the overall trend in the variation of NBO fraction with X_{CaO} are consistent with those expected from composition, those in the calcium aluminosilicate glasses are somewhat different from the predicted values. The presence of NBO in glasses on the charge-balanced join has already been demonstrated (Stebbins and Xu, 1997). On the other hand, the fraction of NBO in the grossularite composition glasses (about 26–27%) appears to be smaller than the predicted value of 33%, possibly because of the presence of $^{[5]}$Al. Indeed, recent Al-27 3QMAS NMR spectra at 17.6 T indicated the presence of about 7–8% $^{[5]}$Al in similar composition glasses (Iuga et al., 2005). A trend of decreasing fraction of NBO with an increase in Al coordination number in aluminosilicates has indeed been reported for aluminosilicate glasses quenched from melts at high pressure (e.g., Yarger et al., 1995; Lee et al., 2004; Allwardt et al., 2005). We note however, that an ^{27}Al 3QMAS NMR spectrum collected at 9.4 T for CAS313 does not provide definite evidence for $^{[5]}$Al (detection limit of about 1–2%). The reason for the difference is likely due to the different radio frequency (RF) power levels of the two experiments (17.6 vs. 9.4 T), as experiments at higher RF field often lead to more signal intensity from larger C_q sites such as $^{[5]}$Al.

The fractions of the various BO clusters provide unique constraints on the degree of framework disorder. For aluminosilicate glasses, this can often be parameterized using the degree of Al avoidance (Q) that varies from 1 (complete Al-avoidance) to 0 (random distribution of Si and Al) (see Lee and Stebbins, 1999; Lee and Stebbins, 2002 for definition). The degree of Al avoidance is also affected by the cation field strength of non-framework cations, ranging from about 0.94 (for Na^+) to 0.75 (for Mg^{2+}) (Lee et al., 2005). Previous quantification of the degree of Al avoidance in calcium aluminosilicate glasses showed that Q varies from 0.8 to 0.875 and does not vary much with Si/Al along the charge-balanced join (Lee and Steb-

bins, 1999; Lee and Stebbins, 2002). However, Q, as manifested in the fractions of BO clusters, could be affected by the degree of polymerization or X_{CaO}. For example, the Q value for CAS223 glasses calculated from the data presented above is about 0.84, which is consistent with values for other calcium aluminosilicate glasses on the charge-balanced join. On the other hand, the Q value for CAS313 is about 0.6, suggesting a greater degree of framework disorder. While the confirmation of this trend requires more systematic study with varying compositions, this effect could result from increasing interaction between network modifying cations and BO clusters, leading to an increase in the extent of disorder (e.g., a more effective compensation of the partial negative charge on Al–O–Al oxygens). Finally, we note again that there is considerable intrinsic uncertainty in the fitting results due to peak overlaps. Thus, although the results shown here can be useful to provide new information on trends of oxygen cluster populations with composition, care must be taken not to draw overly definitive conclusions.

3.3. Insights from quantum chemical molecular orbital calculations

As has been demonstrated in previous O-17 NMR studies of calcium aluminosilicate glasses (Allwardt et al., 2003), NBO in the glasses studied here is predominantly Ca–O–Si, while Al–NBO (Ca–O–Al) appears to be energetically much less favorable, as its concentration is below detection limits. Quantum chemical calculations can provide additional insights on the NBO distributions. Fig. 10 shows the optimized geometry of the model Ca-aluminosilicate clusters, where Ca^{2+} is coordinated by 4 oxygens. The Ca–[O–Al] distance (Fig. 10b) is 2.089 Å and Ca–[O–Si] (Fig. 10c) is about 2.12 Å. Note that Ca clusters with NBO were originally optimized from the cluster without NBO (Fig. 10a) by removing one hydrogen from a terminal Al–O or from a terminal Si–O (Fig. 10c). The calculated energy difference between Al–NBO and Si–NBO at the B3LYP/6-311G(2d,p) level is 108 kJ/mol, suggesting a large energy penalty for the formation of Al–NBO. We note that the accuracy of this model is limited because calculated energies are expected to depend on composition (Si/Al, number of Ca, etc.) and on constraints in optimization. For example, further relaxation of the clusters by eliminating these constraints could lead to lower configuration energies and thus to changes in the energy differences between the clusters. In addition, the cluster sizes are too small to capture some relevant features of the real local structure, particularly the high likelihood that NBO have multiple Ca cation neighbors. While it is desirable to have larger clusters with minimum perturbation by hydroxyl groups, small clusters have often been used to provide *qualitative* interpretation of experimental data as is the case

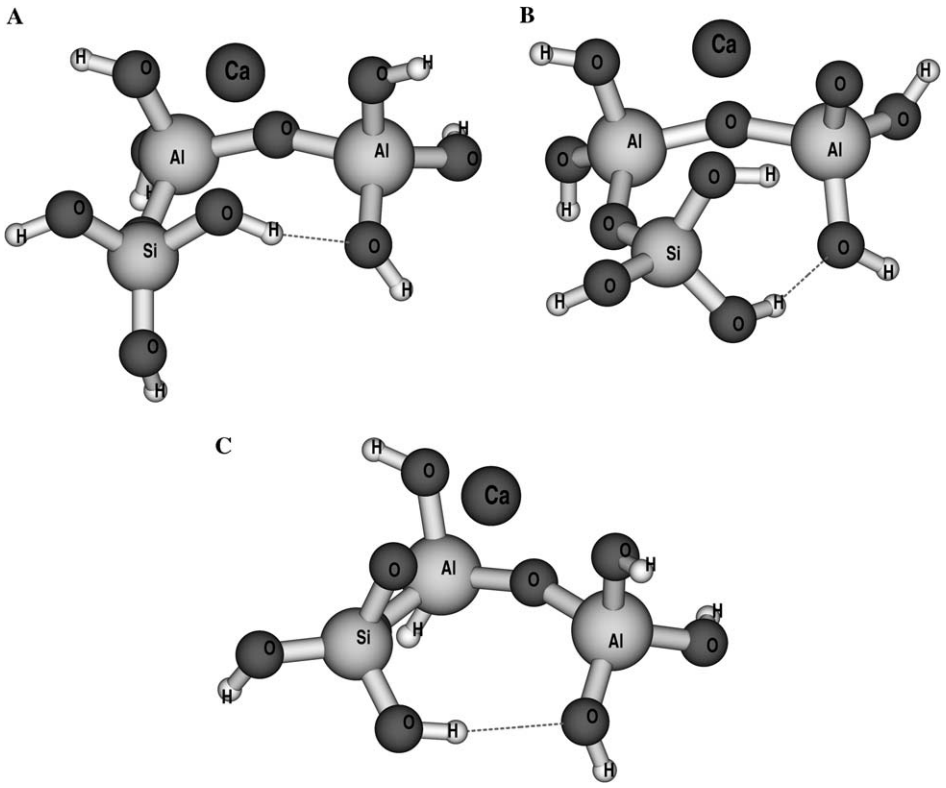

Fig. 10. Model Ca-aluminosilicate clusters. (A) Ca aluminosilicate clusters without non-bridging oxygen ($CaAl_2Si_1O_{2BO}(OH)_8$). (B) Ca-cluster with Al–NBO ($CaAl_2Si_1O_2O_{Al-NBO}(OH)_7$), (C) Ca-cluster with Si–NBO ($CaAl_2Si_1O_{2BO}O_{Si-NBO}(OH)_7$). Note that all the framework cations (Si and Al) are linked by bridging oxygen as is clear from the composition.

here. Despite the utility of small cluster calculations in roughly estimating energy differences, further analysis with larger clusters would provide more realistic atomic structures around NBO and BO with several network modifying cations (e.g., coordination of Ca is close to 6.5 from earlier X-ray and neutron scattering experiments Richet et al., 1993; Zhao et al., 1997; Cormier et al., 2000) and thus yield a more accurate energy penalty for the formation of Al–NBO.

3.4. Implications for macroscopic properties of melts

From the experimental data presented here, insights into the corresponding macroscopic properties can be obtained. While better quantification of oxygen cluster populations (bridging oxygen and NBO) could yield more quantitative macroscopic properties, the trends shown are useful. the trends shown above are helpful in accounting for macroscopic properties (i.e., viscosity) and their microscopic origins. Here, we attempt to obtain composition dependent activation energies of viscous flow from the experimentally measured viscosity data and NBO fractions from O-17 solid-state NMR. As previously reported, the NBO fraction (X_{NBO}) can be directly correlated to the melt viscosity (Mazurin, 1983; Giordano and Dingwell, 2003; Lee, 2005). For instance, a decrease in X_{NBO} of 0.1 along the Ca-silicate binary (from 0.5 to 0.8) results in a almost linear change in viscosity at 1500 °C of about 0.256 log units (Mazurin, 1983). This relationship and the effect of temperature may also be expressed as follows:

$$\left(\frac{\partial \ln \eta}{\partial X_{\mathrm{NBO}}}\right)_T \propto \frac{(E_{\mathrm{NBO}} - E_{\mathrm{BO}})}{kT} \tag{1}$$

Here, η is the viscosity of melts at high temperature where the flow process follows Arrhenian behavior. E_{NBO} and E_{BO} are defined previously to be the activation energy barriers responsible for viscous flow when the system is composed of exclusively NBO and BO, respectively; k is the Boltzman constant. The relationship is derived from Eq. (4) of Lee et al. (2004). Since $E_{\mathrm{NBO}} - E_{\mathrm{BO}}$ is negative, the dependence of viscosity on X_{NBO} increases with decreasing temperature. At lower temperatures, $[\partial \ln \eta / \partial X_{\mathrm{NBO}}]$ is also dependent on $[\partial T_g / \partial X_{\mathrm{NBO}}]$ and on $[\partial F / \partial X_{\mathrm{NBO}}]$, where the derivatives indicate the dependencies of viscosity, glass transition, and fragility (F) on X_{NBO}, respectively. Eq. (1) demonstrates that the relationship between experimentally measured viscosity and NBO fraction from O-17 NMR can potentially yield information about relative magnitudes of E_{NBO} and E_{BO} if there is any compositional dependence. Further modeling of melt properties can utilize the fractions of X_{NBO} (that can be directly determined from experiment) as a model parameter to constrain melt properties quantitatively.

While quantitative assessment on the thermodynamic properties of multi-components melts and glasses is complex and model dependent, our preliminary semi-quantitative calculation of configurational enthalpy in the CS43–CAS223 join using the oxygen cluster populations (Fig. 8) is negative (with minimum in the CAS313) (Lee and Stebbins, 2002). We also note that the fraction of Si–O–Si is probably directly related to the activity of SiO_2 in the glasses and melts, and in turn helps to determine the composition of melts generated in equilbrium with crystalline phases (see Hess, 1995; Lee, 2005 for review and the references therein) in such a way that the silica activity increases with $X_{\mathrm{Si–O–Si}}$. Therefore, the trend observed along the CS43–CAS223 join (constant $X_{\mathrm{SiO_2}}$) as a function of NBO/T (i.e., decreasing $X_{\mathrm{Si–O–Si}}$ with decreasing NBO/T) suggests that the silica activity should decrease from CS43 to CAS223. Such considerations should be useful in helping to understand the effects of multi-component variation in compositions of melts in systems (such as the upper mantle) where silica activity is fixed by host rock mineral assemblages.

Acknowledgments

This project was supported by BK21 program and Young Scientist program from Korean research foundation to SKL (C00076) and by NSF grant EAR 0104926 to J.F.S. We thank Prof. Grandinetti for the RMN software used for NMR processing. We also thank two anonymous reviewers and Dr. B. Poe for critical comments and constructive suggestions.

Associate editor: Brent T. Poe

References

Allwardt, J., Lee, S.K., Stebbins, J.F., 2003. Bonding preferences of non-bridging oxygens in calcium aluminosilicate glass: evidence from O-17 MAS and 3QMAS NMR on calcium aluminate glass. *Am. Mineral.* **88**, 949–954.

Allwardt, J.R., Stebbins, J.F., Schmidt, B.C., Frost, D.J., Withers, A.C., Hirschmann, M.M., 2005. Aluminum coordination and the densification of high-pressure aluminosilicate glasses. *Am. Mineral.* **90**, 1218–1222.

Amoureux, J.P., Fernandez, C., Frydman, L., 1996. Optimized multiple-quantum magic-angle spinning NMR experiments on half-integer quadrupoles. *Chem. Phys. Lett.* **259**, 347–355.

Ashbrook, S.E., Berry, A.J., Wimperis, S., 2002. O-17 multiple-quantum MAS NMR study of pyroxenes. *J. Phys. Chem. B.* **106**, 773–778.

Bak, M., Rasmussen, J.T., Nielsen, N.C., 2000. Simpson: a general simulation program for solid-state NMR spectroscopy. *J. Magn. Reson.* **147**, 296.

Baltisberger, J.H., Xu, Z., Stebbins, J.F., Wang, S., Pines, A., 1996. Triple-quantum two-dimensional ^{27}Al magic-angle spinning nuclear magnetic resonance spectroscopic study of aluminosilicate and aluminate crystals and glasses. *J. Am. Chem. Soc.* **118**, 7209–7214.

Bottinga, Y., Weill, D.F., 1972. The viscosity of magmatic silicate liquids: a model for calculation. *Am. J. Sci.* **272**, 438–475.

Cormier, L., Ghaleb, D., Neuville, D.R., Delaye, J.M., Calas, G., 2003. Chemical dependence of network topology of calcium aluminosilicate glasses: a computer simulation study. *J. Non-Cryst. Solids* **332** (1-3), 255–270.

Cormier, L., Neuville, D.R., Calas, G., 2000. Structure and properties of low-silica calcium aluminosilicate glasses. *J. Non-Cryst. Solids* **274** (1–3), 110–114.

Dirken, P.J., Kohn, S.C., Smith, M.E., Vaneck, E.R.H., 1997. Complete resolution of Si–O–Si and Si–O–Al fragments in an aluminosilicate glass by O-17 multiple-quantum magic-angle-spinning NMR-spectroscopy. *Chem. Phys. Lett.* **266**, 568–574.

Du, L.S., Stebbins, J.F., 2005. Network connectivity in aluminoborosilicate glasses: a high-resolution ^{11}B, ^{17}O, and ^{27}Al NMR study. *J. Non-Cryst. Solids* **351**, 3508–3520.

Dubinsky, E.V., Stebbins, J.F., 2005. Quench rate studies of framework ordering in aluminosilicate glasses: implications for pressure and temperature effects on melt structure. *Eos, Trans. Am. Geophys.* Union Fall meeting.

Dubinsky, E.V., Stebbins, J.F., 2006. Quench rate and temperature effects on framework ordering in aluminosilicate melts. *Am. Mineral.* **91**, 753–761.

Eckert, H., 1992. Structural characterization of noncrystalline solids and glasses using solid state NMR. *Prog. Nucl. Mag. Reson.* **24**, 159–293.

Engelhardt, G., Michel, D., 1987. *High-Resolution Solid-State NMR of Silicates and Zeolites*. Wiley, New York.

Foresman, J.B., Frisch, A., 1996. *Exploring Chemistry with Electronic Structure Methods*. Gaussian Inc.

Frisch, M.J., Trucks, G.W., Schlegel, H.B., Scuseria, G.E., Robb, M.A., Cheeseman, J.R., Zakrzewski, V.G., Montgomery Jr., J.A., Stratmann, R.E., Burant, J.C., Dapprich, S., Millam, J.M., Daniels, A.D., Kudin, K.N., Strain, M.C., Farkas, O., Tomasi, J., Barone, V., Cossi, M., Cammi, R., Mennucci, B., Pomelli, C., Adamo, C., Clifford, S., Ochterski, J., 1998. Gaussian 98, Revision A.11.

Frydman, I., Harwood, J.S., 1995. Isotropic spectra of half-integer quadrupolar spins from bidimensional magic-angle-spinning NMR. *J. Am. Chem. Soc.* **117**, 5367–5368.

Gan, Z.H., Gor'kov, P., Cross, T.A., Samoson, A., Massiot, D., 2002. Seeking higher resolution and sensitivity for NMR of quadrupolar nuclei at ultrahigh magnetic fields. *J. Am. Chem. Soc.* **124**, 5634–5635.

Giordano, D., Dingwell, D.B., 2003. Non-Arrhenian multicomponent melt viscosity: a model. *Earth. Planet. Sci. Lett.* **208**, 337–349.

Hess, P.C., 1995. Thermodynamic mixing properties and structure of silicate melts. In: Stebbins, J.F., McMillan, P.F., Dingwell, D.B. (Eds.), *Structure, Dynamics, and Properties of Silicate Melts*. Mineralogical Society of America, pp. 145–189.

Hwa, L.G., Hwang, S.L., Liu, L.C., 1998. Infrared and Raman spectra of calcium alumino-silicate glasses. *J. Non-Cryst. Solids* **238** (3), 193–197.

Iuga, D., Morais, C., Gan, Z.H., Neuville, D.R., Cormier, L., Massiot, D., 2005. NMR heteronuclear correlation between quadrupolar nuclei in solids. *J. Am. Chem. Soc.* **127** (33), 11540–11541.

Kirkpatrick, R.J., Dunn, T., Schramm, S., Smith, K.A., Oestrike, R., Turner, G., 1986. Magic-angle sample-spinning nuclear magnetic resonance spectroscopy of silicate glasses: a review. In: Walrafen, G.E., Revesz, A.G. (Eds.), *Structure and Bonding in Noncrystalline Solids*. Plenum Press, New York, pp. 302–327.

Kohn, S.C., 2004. NMR studies of silicate glasses. In: Beran, A., Libowitzky, E. (Eds.), *EMU Notes in Mineralogy: Spectroscopic Methods in Mineralogy*, vol. 6, pp. 399–419.

Kohn, S.C., Smith, M.E., Dirken, P.J., van Eck, E.R.H., Kentgens, A.P.M., Dupree, R., 1998. Sodium environments in dry and hydrous albite glasses; improved ^{23}Na solid state NMR data and their implications for water dissolution mechanisms. *Geochim. Cosmochim. Acta* **62**, 79–87.

Kubicki, J.D., Toplis, M.J., 2002. Molecular orbital calculations on aluminosilicate tricluster molecules: Implications for the structure of aluminosilicate glasses. *Am. Mineral.* **86**, 668–678.

Lee, S.K., 2004. The structure of silicate melts at high pressure: Quantum chemical calculations and solid state NMR. *J. Phys. Chem. B.* **108**, 5889–5900.

Lee, S.K., 2005. Microscopic origins of macroscopic properties of silicate melts: implications for melt generation and dynamics. *Geochim. Cosmochim. Acta* **69**, 3695–3710.

Lee, S.K., Cody, G.D., Fei, Y., Mysen, B.O., 2004. The nature of polymerization and properties of silicate glasses and melts at high pressure. *Geochim. Cosmochim. Acta* **68**, 4203–4214.

Lee, S.K., Cody, G.D., Mysen, B.O., 2005. Structure and the extent of disorder in quaternary (Ca–Mg and Ca–Na) aluminosilicate glasses and melts. *Am. Mineral.* **90**, 1393–1401.

Lee, S.K., Musgrave, C.B., Zhao, P., Stebbins, J.F., 2001. Topological disorder and reactivity of borosilicate glasses: ab initio molecular orbital calculations and ^{17}O and ^{11}B NMR. *J. Phys. Chem. B* **105**, 12583–12595.

Lee, S.K., Stebbins, J.F., 1999. The degree of aluminum avoidance in aluminosilicate glasses. *Am. Mineral.* **84**, 937–945.

Lee, S.K., Stebbins, J.F., 2000. The structure of aluminosilicate glasses: high-resolution ^{17}O and ^{27}Al MAS and 3QMAS NMR study. *J. Phys. Chem. B.* **104**, 4091–4100.

Lee, S.K., Stebbins, J.F., 2002. The extent of inter-mixing among framework units in silicate glasses and melts. *Geochim. Cosmochim. Acta* **66**, 303–309.

Lee, S.K., Stebbins, J.F., 2003a. The distribution of sodium ions in aluminosilicate glasses: a high field Na-23 MAS and 3QMAS NMR study. *Geochim. Cosmochim. Acta* **67**, 1699–1709.

Lee, S.K., Stebbins, J.F., 2003b. Nature of cation mixing and ordering in Na–Ca silicate glasses and melts. *J. Phys. Chem. B.* **107**, 3141–3148.

Massiot, D., Fayon, F., Capron, M., King, I., Le Calve, S., Alonso, B., Durand, J.O., Bujoli, B., Gan, Z.H., Hoatson, G., 2002. Modelling one- and two-dimensional solid-state NMR spectra. *Magn. Reson. Chem.* **40**, 70–76.

Masson, C.R., 1977. Anionic constitution of glass-forming melts. *J. Non-Cryst. Solids* **25**, 3–41.

Mazurin, O.V., 1983. *Handbook of Glass Data : Silica Glass and Binary Silicate Glasses*. Elsevier Science, Amsterdam.

McMillan, P.F., Piriou, B., Navrotsky, A., 1982. A Raman spectroscopic study of glasses along the joins silica-calcium aluminate, silica-sodium aluminate, and silica-potassium aluminate. *Geochim. Cosmochim. Acta* **46**, 2021–2037.

Medek, A., Harwood, J.S., Frydman, L., 1995. Mulitple-quantum magic-angle spinning NMR: a new method for the study of quadrupolar nuclei in solids. *J. Am. Chem. Soc.* **117**, 12779.

Merzbacher, C.K.M., Hinggby, A., 1985. ^{29}Si NMR and infrared reflectance spectroscopy of low silica calcium aluminosilicate. *J. Non-Cryst. Solids* **136**, 249–259.

Murdoch, J.B., Stebbins, J.F., Carmichael, I.S.E., 1985. High-resolution ^{29}Si NMR study of silicate and aluminosilicate glasses: the effect of network-modifying cations. *Am. Mineral.* **70**, 332–343.

Mysen, B., 1998. Transport and configurational properties of silicate melts: relationship to melt structure at magmatic temperatures. *Phys. Ear. Planet. Int.* **107**, 23–32.

Mysen, B.O., 1988. *Structure and Properties of Silicate Melts*. Elsevier, Amsterdam.

Mysen, B.O., Richet, P., 2005. *Silicate Glasses and Melts: Properties and Structure (Developments in Geochemistry)*. Elsevier, Amsterdam.

Mysen, B.O., Virgo, D., Kushiro, I., 1981. The structural role of aluminum in silicate melts—a Raman spectroscopic study at 1 atmosphere. *Am. Mineral.* **66**, 678–701.

Navrotsky, A., 1995. Energetics of silicate melts. In: Stebbins, J.F., McMillan, P.F., Dingwell, D.B. (Eds.), *Structure, Dynamics, and Properties of Silicate Melts*. Mineralogical Society of America, pp. 121–143.

Navrotsky, A., Peraudeau, G., McMillan, P., Coutures, J.P., 1982. A thermochemical study of glasses and crystals along the joins silica-calcium aluminate and silica-sodium aluminate. *Geochim. Cosmochim. Acta* **46**, 2039–2047.

Neuville, D.R., Cormier, L., Massiot, D., 2004. Al environment in tectosilicate and peraluminous glasses: A 27Al MQ-MAS NMR, Raman, and XANES investigation. *Geochim. Cosmochim. Acta* **68**, 5071–5079.

Neuville, D.R., Cormier, L., Massiot, D., 2006. Al coordination and speciation in calcium aluminosilicate glasses : effects of composition determined by ^{27}Al MQ-MAS NMR and Raman spectroscopy. *Chem. Geol.* **229**, 173–185.

Oestrike, R., Kirkpatrick, R.J., 1988. ^{27}Al and ^{29}Si Magic angle spinning NMR spectroscopy of glasses in the system anorthite-diopside-forsterite. *Am. Mineral.* **73**, 534–546.

Oglesby, J.V., Zhao, P., Stebbins, J.F., 2002. Oxygen sites in hydrous aluminosilicate glasses: the role of Al–O–Al and H_2O. *Geochim. Cosmochim. Acta* **66**, 291–301.

Petkov, V., Billinge, S.J.L., Shastri, S.D., Himmel, B., 2000. Polyhedral units and network connectivity in calcium aluminosilicate glasses from high-energy X-ray diffraction. *Phys. Rev. Lett.* **85**, 3436–3439.

Richet, P., Neuville, D.R., 1992. Thermodynamics of silicate melts: configurational properties. In: Saxena, S.K. (Ed.), *Thermodynamic data*. Springer, New York, pp. 132–161.

Richet, P., Robie, R.A., Hemingway, B.S., 1993. Entropy and structure of silicate glasses and melts. *Geochim. Cosmochim. Acta* **57**, 2751–2766.

Stebbins, J.F., Du, L.-S., Kroeker, S., Neuhoff, P., Rice, D., Frye, J., Jakobsen, H.J., 2002. New opportunities for high-resolution solid-state NMR spectroscopy of oxide materials at 21.1 and 18.8 Tesla fields. *Solid State Nucl. Magn. Reson.* **21**, 105–115.

Stebbins, J.F., Lee, S.K., Oglesby, J.V., 1999. Al–O–Al oxygen sites in crystalline aluminates and aluminosilicate glasses: high-resolution oxygen-17 NMR results. *Am. Mineral.* **84**, 983–986.

Stebbins, J.F., McMillan, P.F., Dingwell, D.B., 1995. Structure, Dynamics, and Properties of Silicate Melts. In: Ribe, P. (Ed.), *Reviews in Mineralogy*, vol. 32. Mineralogical Society of America.

Stebbins, J.F., Oglesby, J.V., Lee, S.K., 2001. Oxygen site in silicate glasses: a new view from oxygen-17 NMR. *Chem. Geol.* **173**, 63–75.

Stebbins, J.F., Oglesby, J.V., Xu, Z., 1997. Disorder among network modifier cations in silicate glasses: new constraints from triple-quantum oxygen-17 NMR. *Am. Mineral.* **82**, 1116–1124.

Stebbins, J.F., Xu, Z., 1997. NMR evidence for excess non-bridging oxygen in aluminosilicate glass. *Nature* **390**, 60–62.

Stein, D., Spera, F., 1995. Molecular dynamic simulations of liquids and glasses in the system $NaAlO_2$–SiO_2 methodology and melt structures. *Am. Mineral.* **80**, 417–431.

Toop, G.W., Samis, C.S., 1962. Some new ionic concepts of silicate slags. *Can. Met. Quart.* **224**, 129–156.

Toplis, M.J., Kohn, S.C., Smith, M.E., Poplett, I.J.F., 2000. Fivefold-coordinated aluminum in tectosilicate glasses observed by triple quantum MAS NMR. *Am. Mineral.* **85**, 1556–1560.

Tossell, J.A., 1993. A theoretical study of the molecular basis of the Al avoidance rule and of the spectral characteristics of Al–O–Al linkages. *Am. Mineral.* **78**, 911–920.

Tossell, J.A., Cohen, R.E., 2001. Calculation of the electric field gradients at 'tricluster'-like O atoms in the polymorphs of Al_2SiO_5 and in aluminosilicate molecules: models for tricluster O atoms in glasses. *J. Non-Cryst. Solids* **286**, 187–199.

Wu, G., Rovnyank, D., Sun, B., Griffin, R.G., 1996. High-resolution multiple quantum MAS NMR spectroscopy of half-integer quadrupolar nuclei. *Chem. Phys. Lett.* **249**, 210–217.

Xue, X., Stebbins, J.F., Kanzaki, M., 1994. Correlations between O-17 NMR parameters and local structure around oxygen in high-pressure silicates and the structure of silicate melts at high pressure. *Am. Mineral.* **79**, 31–42.

Yarger, J.L., Smith, K.H., Nieman, R.A., Diefenbacher, J., Wolf, G.H., Poe, B.T., McMillan, P.F., 1995. Al coordination changes in high-pressure aluminosilicate liquids. *Science* **270**, 1964–1967.

Zhao, J., Gaskell, P.H., Cormier, L., Bennington, S.M., 1997. Vibrational density of states and structural origin of the heat capacity anomalies in $Ca_3Al_2Si_3O_{12}$ glasses. *Physica B* **241**, 906–908.